
Proceedings Paper:
Ashworth, S., Fairclough, J.P.A., Sharman, A.R.C. et al. (4 more authors) (2019) Varying CFRP workpiece temperature during slotting : effects on surface metrics, cutting forces and chip geometry. In: Kerrigan, K., Mativenga, P. and El-Dessouky, H., (eds.) Procedia CIRP. 2nd CIRP Conference on Composite Material Parts Manufacturing, 10-11 Oct 2019, Sheffield, UK. Elsevier , pp. 37-42.

https://doi.org/10.1016/j.procir.2019.09.021

Available online at www.sciencedirect.com

ScienceDirect

Procedia CIRP 85 (2019) 36–41

www.elsevier.com/locate/procedia

2nd CIRP Conference on Composite Material Parts Manufacturing (CIRP-CCMPM 2019)

Varying CFRP workpiece temperature during slotting: Effects on surface metrics, cutting forces and chip geometry

Sam Ashworth[a,b,*], J. Patrick A. Fairclough[b], Adrian R C Sharman[c], James Meredith[d], Yoshihiro Takikawa[e], Richard Scaife[c], Kevin Kerrigan[c]

[a]*Industrial Doctorate Centre in Machining Science, Advanced Manufacturing Research Centre with Boeing, University of Sheffield, Rotherham, S60 5TZ, UK*
[b]*Department of Mechanical Engineering, The University of Sheffield, Sheffield, S1 3JD, UK*
[c]*Advanced Manufacturing Research Centre with Boeing, The University of Sheffield, Rotherham S60 5TZ, UK*
[d]*WMG, International Manufacturing Centre, University of Warwick, Coventry, CV4 7AL, UK*
[e]*OSG Corporation,3-22 Honnogahara, Toyokawa, Aichi, 442-8543, Japan*

* Corresponding author. Tel.: +44-796-902-3481; *E-mail address:* sam.ashworth@sheffield.ac.uk

Abstract

Carbon fibre reinforced thermoset polymer (CFRP) components are typically edge trimmed using a milling process to achieve final part shape. During this process the material is subject to significant heating at the tool-workpiece interface. Damage due to heating is fibre orientation specific; for some orientations it can lead to matrix smearing, potentially hiding defects and for others it can increase pullout. Understanding these relationships is critical to attaining higher throughput by edge milling. For the first time this study focuses on active heating of the CFRP rather than passive measurement, through use of a thermocouple controlled system to heat a CFRP workpiece material from room temperature (RT) up to 110 °C prior to machining. Differences in cutting mechanisms for fibres oriented at 0, 45, 90 and -45° are observed with scanning electron microscopy (SEM), and quantified with using focus variation with an increase of 89.9% S_a reported between RT and 110°C CFRP panel pre-heating. Relationships to cutting forces through dynamometer readings and tool temperature through infra-red (IR) measurements are also made with a novel optical method to measure cut chips presented. Results show an increase in chip length and width for increasing cutting temperature from RT to 110°C (3.39 and 0.79 µm for length and width, respectively). This work improves current understandings of how the cutting mechanism changes with increased temperature and suggests how improved milling throughput can be achieved.

Peer-review under responsibility of the scientific committee of the 2nd CIRP Conference on Composite Material Parts Manufacturing.

Keywords: Composite; Machining; Thermal effects; Damage; Surface analysis

1. Introduction

A subtractive method of material removal such as edge milling can be used to achieve final CFRP net shape [1]. Challenges in CFRP machining remain due to the anisotropic two phase nature and fibre direction specific chip formation methods which lead to complex damage mechanisms [2].

Following the milling process, the quality of the part is typically inspected (e.g. R_a or S_a, the arithmetic mean of the micro-scale peaks and valleys of a surface in a 2D or 3D sense [3]) in order to quantify surface defects such as fibre pullout, delamination, matrix smearing or burning [4-6]. Some of these damage types are dependent on temperature during cutting [7, 8]. Matrix smearing is a particular issue for CFRP machining due to the potential for degradation of edge-of-part properties, particularly in aerospace primary structures. Smearing occurs when the fully cured and cross-linked polymer resin state transitions, via increased thermal excitation, into its glass transition temperature (Tg) range at the tool-workpiece interaction. If onset Tg is exceeded, constituents of the polymer matrix, including base resin, curing agent, hardener, inhibitor and plasticiser, can become rubbery (thermoset) or melt (thermoplastic) and, given enough pressure during cutting, smear over the surface of the cut fibres in addition to changing the orientation-specific

2212-8271
Peer-review under responsibility of the scientific committee of the 2nd CIRP Conference on Composite Material Parts Manufacturing.
10.1016/j.procir.2019.09.021

cutting mechanism, a particular issue for fibres oriented at 45° and 90° to the cutting edge [9, 10].

Whilst numerical methods of observing temperature at the tool-workpiece interaction zone have been successful [11], experimental analysis has been limited to the use of thermocouples (TCs) and IR imaging. Whilst steps have been made to improve the observation of the tool-workpiece interaction zone by embedding TCs in the tool [8, 12, 13], the method does not capture temperature effects at the exact point of interaction without further numerical analysis. In addition to tool based TCs, embedded TCs in the material [14] have also be extensively used but due to poor response rates the temperature at the surface of cutting cannot be captured. IR imaging has also been used to observe cutting temperatures and the effects of surface quality [10]. IR has the disadvantage of chip ejection obscuring the trimmed edge and/or the tool when attempting to observe the cutting zone.

By changing the temperature difference between tool and workpiece by using a novel method to adjust the CFRP temperature a fundamental difference in heat flow will occur. Wang *et. al.* [15] note that the total heat energy (Q_{total}) in the cutting interface/heat partition zone is the sum of the workpiece, tool and chip; Q_{CFRP}, Q_{Tool} and Q_{Chip} heat energies respectively (Equation (1)). A change to the temperature of the CFRP workpiece will, through application of Fourier's law, result in a different CFRP heat energy, Q_{CFRP}.

$$Q_{Total} = Q_{CFRP} + Q_{Tool} + Q_{Chip} \quad (1)$$

The high level of uncertainty of temperature measurement in CFRP machining related to instantaneous thermal excitation at the cutting interface and temperatures generated at different cuttings speeds and feeds is difficult to study. Therefore, direct heating of the CFRP panel to change the thermal excitation state of the whole system may provide additional understanding of the cutting mechanisms and chip formation methods. The information could be used to improve milling output to meet increasing CFRP demand within the composites industry [16].

Whilst chip roots have been analysed using quick-stop techniques [17] and by optical and scanning electron microscopy analysis [18, 19], it is noted that limited information exists on analysis of the machined chips themselves, in particular for machining at different temperatures and for woven CFRP material.

This experiment aims to complete machining at different temperatures with a setup to globally exceed the glass transition of CFRP resin during edge milling. As the limitations of direct workpiece tool interactions are not experimentally viable options, the effects of differing starting temperatures of the workpiece material are assessed through dynamometer, focus variation, SEM and for the first time chip analysis methods.

2. Experimental setup

2.1. CFRP panel manufacture and characterisation

A single 300 x 300 x 3 mm CFRP panel with a $[((0,90)/(+45,-45))_3/(0,90)]$s lay-up using T300 2x2 woven material (Sigmatex, UK) and a resin system consisting of DGEBF PY306 epoxy (Huntsman, UK), TETA hardener (Sigma Aldrich, UK) (100:15.2 by mass) was manufactured using an RTM process and characterised as per Ashworth *et. al.* [9] and Ashworth *et. al.* [20].

Fibre, resin and void content were found to be 58.2, 41.6 and 0.2%, respectively using optical methods of analysis. The tan delta Tg of the material was determined as 115.2 °C by dynamic mechanical analysis using a PerkinElmer DMA8000. A PerkinElmer Diamond differential scanning calorimeter was used to calculate endothermic heat flow of the resin system which presented a cure value of 99.9%. This is relevant as no additional post curing or micromechanical property changes are expected during the CFRP preheating and machining method.

2.2. Milling equipment

Figure 1 shows the machining setup of this study. A MAG Cincinnati CFV 3-axis milling machine was used with a BT-40 spindle and an ER collet. A Kistler 9139AA dynamometer plate, 5070A12100 8 channel charge amplifier and DAQ was clamped to the machine bed. An epoxy insulator block was clamped to the dynamometer followed by clamping of a custom aluminium fixture block. Finally the CFRP panel was placed on the fixture and 9x L-brackets used to clamp the CFRP panel. The fixture allows 300 mm of full slot milling along 9 rows where the CFRP has an overhang of 0.5 mm in front and behind the brackets where dry, conventional milling was completed (as per Figure 3 a)).

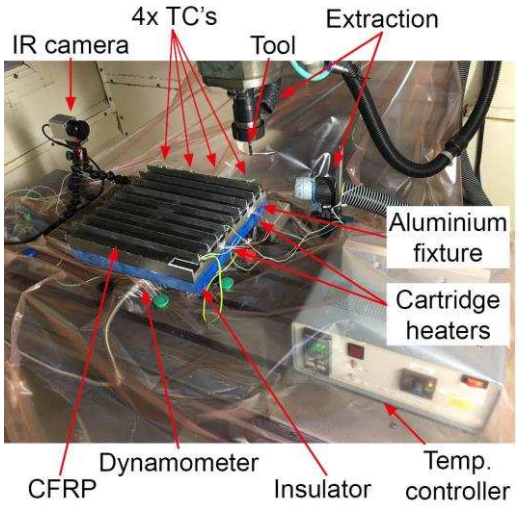

Figure 1 – Machining setup detailing dynamometer, insulator, CFRP fixture, CFRP panel and bracket layers to make up the machining fixture with temperature controller, 4x cartridge heaters and 4x thermocouples with IR camera forming the temperature control and monitoring setup

The CFRP panel was machined at RT and then in increments of 10 °C up to a maximum of 110 °C. The workpiece was heated to such high temperatures in addition to the heat introduced by the tool passing in order to exceed Tg during cutting. The aluminium fixture block is heated by 4x, 500 W, 10 mm diameter, 100 mm long cartridge heaters which were lubricated with 2.9 W/mK silicone grease with 2 inserted per side of the aluminium fixture. Temperature was controlled with four 0.5 mm k-type TCs placed in 0.5 mm diameter, 1.5 mm deep holes at even locations on the CFRP

panel, 0.5 mm from the 18 planned milling locations (Figure 1 and Figure 3 a)). TCs set to a 60 Hz sampling rate were connected to the control unit and a PicoLog TC-08 recorder. Between each 10 °C increment the panel was left to reach an even temperature distribution for half an hour. A maximum variation of 1.9 °C across all four TCs throughout the experiment was found.

All machining was completed with a pre-worn (2.5m linear cutting distance) diamond coated burr style tool (OSG Corporation, UK) as per Table 1 based on manufacturer's recommendations. The DIA-BNC tool is a fine nicked router designed for CFRP trimming with the nick and flute form designed to eliminate uncut fibres and delamination. The DIA-BNC tool has a double helix, each at 15° with a relief and rake angle of 18° and 8°, respectively.

Table 1 – Machining parameters

Tool	No. teeth	Tool diameter (mm)	Cutting speed (m/min)	Feed per tooth (mm/tooth)	Feed per revolution (mm/rev)
DIA-BNC	8	6	179	0.015	0.12

The dynamometer setup utilises total power, U_T, as a metric to capture cutting forces across the 300 mm cut in a convenient way as described in Ashworth *et. al.* [9] and presented in Equation (2) where F is the cutting force, x is the linear distance milled and V is the volume of material removed.

$$U_T = \frac{\int F_x dx + \int F_y dx + \int F_z dx}{V} \quad (2)$$

An Optris PI 450 IR camera was positioned at the end of the 300mm cut to capture maximum tool temperature, away from chip ejection which was found to obscure accurate tool readings. The aluminium fixture and clamping brackets were sprayed black to prevent reflections which could potentially change IR readings. Emissivity settings for each cut were based on calibration trials where the tool was heated from 100 to 200 °C, measured with a TC and the emissivity value of the IR camera altered until temperature was recorded correctly. It was noted that a range of emissivity values were required to correctly match the TC reading depending on tool temperature so an average value of 0.93 chosen. Therefore IR tool temperature readings should be used as a guide only however whilst the limitations on providing the exact temperature are understood, any trends observed by the camera are still valid.

2.3. Post-machining assessment

The surface quality of samples was observed at 8 locations for each temperature in line with the TC location both in front and behind clamping brackets (Figure 3 a)) i.e. at 60, 120, 180 and 240 mm each side of the coupon to account for temperature increases during the cutting process as the tool heats from its original pre-cut temperature. Areal surface scanning was conducted using an Alicona G5 focus variation system using 10 x magnification. Exposure was set to 7.25 ms and contrast set to 0.7 with vertical resolution and lateral resolution set to 200 nm and 1 µm respectively. A scanning area of 5 x 3 mm (complete thickness of sample) was taken. λ_c, the cut-off wavelength which separates roughness from waviness was set to 2.5 mm in accordance with BS EN ISO 4288 [21]. S_a was used as a comparator for machined specimens.

A ThermoFisher Scientific FEI Inspect F SEM was used to assess damage at high magnification on the machined edge. Sputter gold-coated samples were mounted on 32mm diameter stubs using Electrodag 1415 silver conducting adhesive (Agar Scientific, UK). A 5 kV accelerometer voltage and a level 3 spot size were used.

Chips from the machining process were collected from the CFRP panel and aluminium fixture between each cut. The panel, fixture and surrounding area were then cleaned using the extraction system and a brush to remove potential contamination of machined particles between cuts.

The morphology of CFRP chips from RT, 60 and 110 °C machining trials were analysed using a Malvern Morphologi G3 through the static image analysis method. A sample volume of 5 mm^3 was dispersed using the in-built dry powder dispersion unit at a pressure of 1 bar and injection time of 10 ms. Particles were allowed to settle under gravity for 120 s inside the closed unit. The dispersion parameters were carefully selected to avoid damage to fragile particles whilst ensuring that agglomerated material was uniformly dispersed. Images were taken automatically at 5x magnification with the sample illuminated diascopically. Imaged particles with less than 100 pixels were discounted from the shape analysis and an average of 50,000 particles were analysed.

3. Results

3.1. Temperature measurements

Figure 2 shows the tool temperature IR measurement observed at the end of each 300 mm cut for temperatures ranging from RT to 110°C. In order to observe if there is a trend between data points, linear regression is applied to tool and CFRP panel temperature in Figure 2 yielding a p-value <0.001 suggesting a strong linear correlation between increasing CFRP temperature and decreasing IR tool temperature.

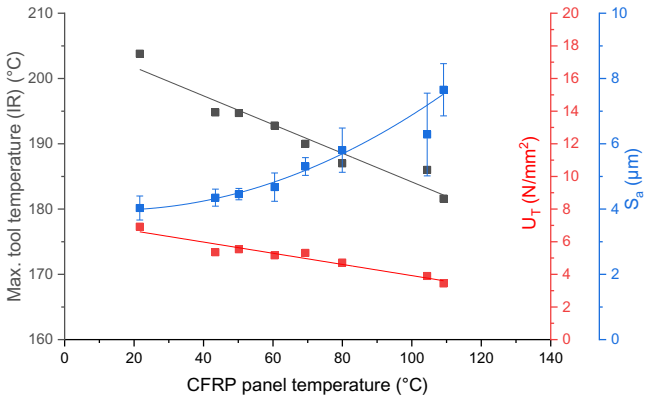

Figure 2 – IR tool temp., U_T and S_a measurements during edge milling of CFRP heated from RT to 110°C with linear (tool temp., U_T) and non-linear (S_a) regression fitting. IR tool temp. and U_T mean values of two samples per temperature, S_a mean from eight samples, ±1 SD presented

This inversely proportional relationship suggests that the

softer matrix requires less cutting force. Therefore, less work is transferred to the tool as heat due to the lower frictional forces as the matrix becomes less brittle [22]. It is also shown that the tool exceeds the Tg of the material (115.2 °C) for all CFRP starting temperatures. Whilst the heat transfer from the tool to the material is likely to be minimal due to the high feed rate and previously noted heat sink of surrounding material, it is still likely that the surface of the machined specimen has exceeded the CFRP Tg. The thermal conductivity of CFRP increases at higher temperatures [23] which conducts heat away from the tool into the specimen during machining leading to decreasing tool temperature.

The removal of a small section of the panel for DMA analysis exposed a portion of the panel where only a small amount of material would be left when trimmed. Figure 3 highlights where approximately 1 mm of overhang from the cutting path was trimmed at a CFRP starting temperature of 50°C, burning the matrix (observed smoke) and leaving unsupported fibres. This suggests that the Tg of the material is exceeded and pyrolysis (approx. 305 °C [24]) has been achieved. For coupons cut in this experiment it is therefore hypothesised that the material behind a larger tool immersion depth acts as a heat sink, preventing pyrolysis such as that seen in Figure 3.

a)

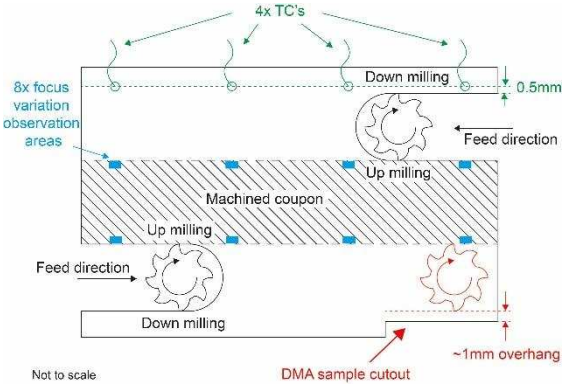

b)

Figure 3 – a) Up milling configuration for flexural coupons (black), focus variation assessment locations (blue), TC location (green), small overhang (red) used to produced b) fibres exposed by pyrolysis of the epoxy matrix during CFRP milling at starting temperature of 50 °C

During the trial phase of the setup it was observed that the edges of the trimmed samples could not be imaged directly due to the positioning of the clamping brackets which stopped edge-on measurements. However, the first edge at the end of the aluminium fixture could be observed (ε set to 0.98 and calibrated with TC). Whilst the chip pile dominates the IR image and the edge cannot be observed directly, Figure 4 highlights the resulting chip pile immediately after tool passing (and chip settling) for RT workpiece starting temperature.

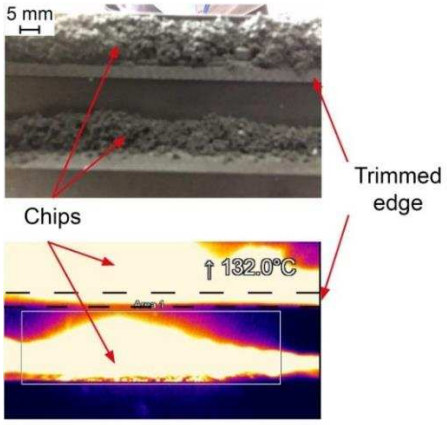

Figure 4 – a) optical image of chip pile which has settled post IR observation and b) corresponding IR image showing 132 °C chip temperature, immediately after tool passing for RT milling

With the evidence presented in Figure 3 and Figure 4, it is reasonable to assume that trimming operations for starting temperatures greater than and equal to RT, will exceed the material Tg at the cutting interface. The impact of the heat that surpasses Tg will be explored in post machining assessment of the coupons.

3.2. Dynamometer measurements

The average U_T for each side of coupon cutting is given in Figure 2. U_T decreases as temperature increases with a linear regression model providing a p-value <0.001 suggesting a strong linear statistical relationship between initial temperature of the CFRP panel and U_T. As noted previously, the tool appears to be heating less during machining of higher temperature preheated CFRP which is also supported by Figure 2 which suggests that less power is transferred between tool and workpiece which would result in lower tool temperature.

3.3. Surface quality measurements

Figure 2 shows the surface quality in terms of S_a for samples milled with different CFRP starting temperatures. It can be seen that mean S_a increases with higher CFRP starting temperatures and the S_a value at 110°C represents an increase of 89.8% compared to RT. Whilst tool temperature and U_T have shown linear trends, a non-linear 2nd order polynomial fits the relationship between CFRP preheating temperature and S_a with a p-value <0.001 confirming a statistically significant relationship through ANOVA. The improvement of S_a for lower CFRP preheating temperatures is reflected in current trends investigating the use of cryogenic cooling [25] where R_a improvements have been noted due to lower cutting temperatures.

Where S_a is set to a response with U_T and IR tool temperature set as variables, both have statistically significant links (p-value <0.001). This is contradictory to expectations where lower forces should correspond to better surfaces however as S_a increases, the U_T and IR tool temperature decrease. This suggests that higher cutting forces allow an improvement in S_a. To achieve higher cutting forces the temperature of the panel must be lower to allow for increased matrix stiffness. An increase in cutting force,

i.e. lower CFRP preheating temperature, would also correspond to an increase in tool temperature which improves results. Therefore an increased temperature in the tool rather than the CFRP panel would be advantageous. This is understandable; as the matrix remains cooler it is able to support fibres so they can be fractured closer to the cutting edge. Conversely, as tool temperature increases it only affects the matrix locally, i.e. close to the surface, whereas CFRP panel preheating changes the global matrix properties, not just the surface. However, this must be considered against the sub-surface damage which at this moment is an unknown and appears to be more important for lower CFRP panel preheating temperatures.

Figure 5 elucidates a surface height topography comparison between samples machined at RT and 110 °C. Visually an increase in the depth range of valleys and peaks can be seen. Larger craters in the -45° orientation of fibres to the cutting edge occurs for all preheated CFRP temperatures which matches literature expectations of large scale pullout [26]. The increase in CFRP preheating temperature has caused a global softening of the matrix. When fibres at 45° to the cutting edge are trimmed at RT, local matrix heating allows the fibres to be pushed beneath the tool. When preheated to 110°C the tool interaction causes matrix softening to a greater depth allowing the fibres to be pushed further beneath the cutting edge of the tool leading to increased spring-back.

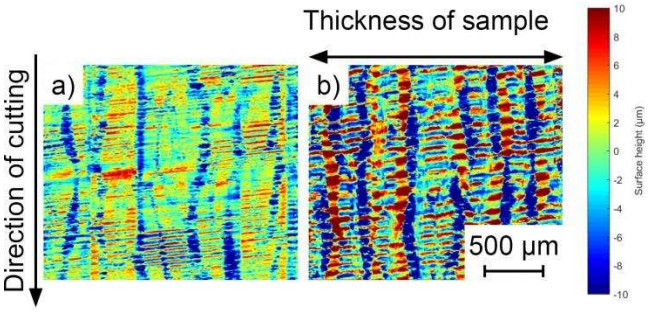

Figure 5 –Surface height topography for a) RT and b) 110 °C CFRP material obtained through focus variation

The non-linear relationship of S_a to CFRP preheating temperature suggests that the surface is improved at lower preheating temperatures. However it is observed that matrix smearing decreases with increasing temperature and machining at lower preheating temperatures appears to increase smearing in the 45 and 90° plies. At lower CFRP preheating temperatures, the greater smearing coincides with an improvement in the -45° orientation due to less pullout. This suggests that surface metrics may not be appropriate i.e. whilst the surface appears better for machining at lower temperatures, the matrix is smeared over 45 and 90° plies where defects may in fact be larger. This calls into question the efficacy of the areal metric parameters where micro x-ray computed tomography (XCT) or other sub-surface method may be more appropriate to measure defects.

Figure 6 shows the effects of machining at 110 °C whereby fibres in the 0° direction are comparable to those in literature [9]. The cutting mechanics for 45, 90 and -45° at temperatures above RT differ from previously noted literature [9]. What is additionally noted is the lack of matrix smearing across fibres at 45 and 90°. It is proposed that the machining at elevated CFRP panel temperatures causes fibre bounce back, exposing the fibres above the matrix. In this way the matrix is no longer smeared over the fibres. This is more prevalent for fibres at 90° but the high magnification SEM micrographs show that the fracture of fibres is not a constant height. This adds further need for sub surface measurement of machining operations at RT with matrix smearing as the differing depth level of fibre cutting may be hidden by matrix smearing.

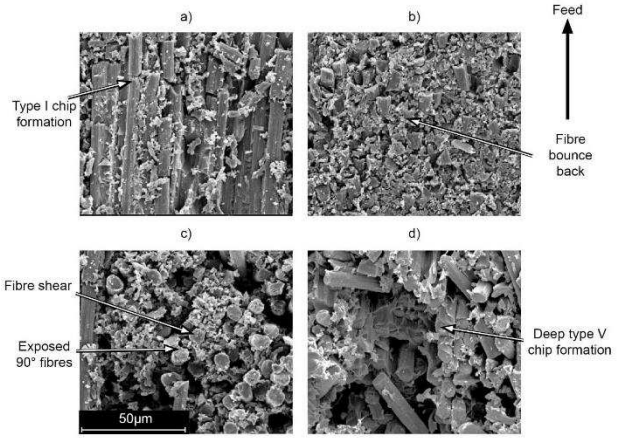

Figure 6 – Micrographs at 2500 x magnification at a) 0, b) 45, c) 90 and d) -45° fibre orientations to the cutting edge for sample milled at 110 °C CFRP preheating temperature with cutting formations noted

3.4. Machined chip size analysis

Table 2 – Mean values for particle length and width from milling

Sample temperature (°C)	Mean Length (µm)	Mean Width (µm)
21.65	20.39	12.88
60.48	21.15	13.15
109.14	23.78	13.67

The mean values from chip analysis are shown in Table 2. Length and width of chips increase according to the temperature of milling and statistical t-tests between the groups all have p-values <0.001 suggesting a high degree of correlation between temperature and particle size. This suggest that the chip is dominated by fibre material; if the matrix which supports the fibres is more ductile as it becomes close to or exceeds the glass transition temperature and supports the fibres less, fibres in all orientations, with the exception of 0° will not be cleanly cut by the tool edge and will be subject to more bending forces leading to fracture further down the fibre length, away from the tool cutting edge. This potentially changes chip formation methods noted in literature. This method of matrix softening leading to larger chips is also supported by the surface topography of the machined sample shown in Figure 5 and 6.

4. Conclusions

Using the novel experimental technique it was observed that S_a values of CFRP preheated to 110°C increased by 89.8% compared to RT. A non-linear statistical link (p-value <0.001) was observed for the trend between S_a and CFRP panel preheating temperature. Statistical links between

variables of dynamometer (U_T) and IR tool temperature immediately after cutting were identified with the response of CFRP panel pre-heating temperature (p-values <0.001).

The cutting mechanisms of 45, 90 and -45° fibres oriented to the tool change significantly with increasing CFRP panel preheating. Unlike RT cutting operations where only a small surface layer of matrix is altered by smearing in the 45 and 90° directions, cutting at elevated CFRP panels temperatures causes global matrix softening. The less stiff matrix is therefore unable to support the fibres close to the cutting edge leading to increased fibre bounce back in the 45 and 90° fibre orientation. Whilst pullout of -45° fibres is evident in RT milling, the fracture zone is further ahead and deeper from the cutting edge for elevated temperature milling. The difference in cutting mechanism for CFRPs is reported for the first time through optical chip analysis which shows increases in mean chip length and width (3.39 and 0.79 µm, respectively) which is statistically different between CFRP pre-heating temperatures of RT, 60 and 110°C (p-value <0.001).

Changing the CFRP panel temperature is not a preferred method of controlling temperature effects with tool temperatures suggested as a more optimal method of control due to the IR observations of the tool at the end of cuts. When S_a was correlated against tool temperature it was noted that higher temperatures produced improved S_a values. It is proposed that the local effects of increased tool temperature produce improved S_a results compared to the global matrix effects of heating the CFRP panel. However whilst it was observed that lower CFRP preheating allowed improved S_a results the effects on sub-surface defects are not understood and XCT or alternative sub-surface investigations should be completed. Further testing should investigate if keeping the CFRP material or the cutting tool itself cool is better in terms of improving surface quality and mechanical performance.

The novel CFRP heating method and observation of observed surfaces has provided new insight into the cutting mechanisms of high temperatures where the Tg of the matrix is exceeded.

5. Acknowledgements

The authors would like to acknowledge the EPSRC Industrial Doctorate Centre in Machining Science (EP/L016257/1) for the funding of this work and to the OSG Corporation for the supply of tools. Thanks are also extended to staff of the Factory of the Future, AMRC.

6. References

[1] Sheikh-Ahmad, J., *Machining of polymer composites*: Springer. 2008. p. 37-62
[2] Hocheng, H., Puw, H.Y., Yao, K.C., Machinability of some fiber-reinforced thermoset and thermoplastics in drilling. *Materials & manufacturing processes*, 1993. **8**(6): p. 653. http://dx.doi.org/10.1080/10426919308934872
[3] Stout, K.J., et al., *The development of methods for the characterization of roughness in three dimensions*. Luxembourg: Commission of the European communities. 1993. p. 216-246.
[4] Haddad, M., et al., Study of trimming damages of CFRP structures in function of the machining processes and their impact on the mechanical behavior. *Composites Part B: Engineering*, 2014. **57**: p. 136. http://dx.doi.org/10.1016/j.compositesb.2013.09.051.
[5] Duboust, N., et al., An optical method for measuring surface roughness of machined carbon fibre reinforced plastic composites. *Journal of Composite Materials*, 2015. **51**(3): p. 289. https://doi.org/10.1177/0021998316644849
[6] Kerrigan, K.,G.E. O'Donnell, On the relationship between cutting temperature and workpiece polymer degradation during CFRP edge trimming. *Procedia CIRP*, 2016. **55**: p. 170. https://doi.org/10.1016/j.procir.2016.08.041.
[7] El-Hofy, M.H., et al., Factors affecting workpiece surface integrity in slotting of CFRP. *Procedia Engineering*, 2011. **19**: p. 94. http://dx.doi.org/10.1016/j.proeng.2011.11.085.
[8] El-Hofy, M.H., et al., Tool temperature in slotting of CFRP composites. *Procedia Manufacturing*, 2017. **10**: p. 371. https://doi.org/10.1016/j.promfg.2017.07.007.
[9] Ashworth, S., et al., Effects of machine stiffness and cutting tool design on the surface quality and flexural strength of edge trimmed carbon fibre reinforced polymers. *Composites Part A: Applied Science and Manufacturing*, 2019. **119**: p. 88. https://doi.org/10.1016/j.compositesa.2019.01.019.
[10] Ghafarizadeh, S., G. Lebrun,J.-F. Chatelain, Experimental investigation of the cutting temperature and surface quality during milling of unidirectional carbon fiber reinforced plastic. *Journal of Composite Materials*, 2015: https://doi.org/10.1177/0021998315587131
[11] Battaglia, J.L., et al., Solving an inverse heat conduction problem using a non-integer identified model. *International Journal of Heat and Mass Transfer*, 2001. **44**(14): p. 2671. https://doi.org/10.1016/S0017-9310(00)00310-0.
[12] Kerrigan, K., et al., An integrated telemetric thermocouple sensor for process monitoring of CFRP milling operations. *Procedia CIRP*, 2012. **1**: p. 449. http://dx.doi.org/10.1016/j.procir.2012.04.080.
[13] Kerrigan, K.,G.E. O'Donnell, Temperature measurement in CFRP milling using a wireless tool-integrated process monitoring sensor. *International Journal of Automation Technology*, 2013. **7**(6): p. 742.
[14] Davies, M.A., et al., On the measurement of temperature in material removal processes. *CIRP Annals*, 2007. **56**(2): p. 581. https://doi.org/10.1016/j.cirp.2007.10.009.
[15] Wang, F.-J., et al., Heat partition in dry orthogonal cutting of unidirectional CFRP composite laminates. *Composite Structures*, 2018. **197**: p. 28. https://doi.org/10.1016/j.compstruct.2018.05.040.
[16] Farries, P.,C. Eyers, *Aviation co2 emissions abatement potential from technology innovation*. 2008, Qinetiq.
[17] Koplev, A., A. Lystrup,T. Vorm, The cutting process, chips, and cutting forces in machining CFRP. *Composites*, 1983. **14**(4): p. 371. http://dx.doi.org/10.1016/0010-4361(83)90157-X.
[18] Hocheng, H., Puw, H.Y., Huang, Y., Preliminary study on milling of unidirectional carbon fiber reinforced plastics. *Composite Manufacturing*, 1993. **4**: p. 103. https://doi.org/10.1016/0956-7143(93)90077-L
[19] Voß, R., et al., Chip root analysis after machining carbon fiber reinforced plastics (CFRP) at different fiber orientations. *Procedia CIRP*, 2014. **14**: p. 217. https://doi.org/10.1016/j.procir.2014.03.013.
[20] Ashworth, S., et al., Mechanical and damping properties of resin transfer moulded jute-carbon hybrid composites. *Composites Part B: Engineering*, 2016. **105**: p. 60. http://dx.doi.org/10.1016/j.compositesb.2016.08.019.
[21] ISO 4288:1998, *Geometric product specification (GPS) — surface texture — profile method: Rules and procedures for the assessment of surface texture*
[22] Puck, A., Schürmann, H., Failure analysis of frp laminates by means of physically based phenomenological models. *Composites Science and Technology*, 2002. **62**(12-13): p. 1633. https://doi.org/10.1016/S0266-3538(01)00208-1
[23] Pilling, M.W., et al., The thermal conductivity of carbon fibre-reinforced composites. *Journal of Materials Science*, 1979. **14**(6): p. 1326. https://doi.org/10.1007/BF00549304.
[24] Gong, X., et al., Decomposition mechanisms of cured epoxy resins in near‐critical water. *Journal of Applied Polymer Science*, 2015. **132**(11). https://doi.org/10.1002/app.41648
[25] Morkavuk, S., et al., Cryogenic machining of carbon fiber reinforced plastic (CFRP) composites and the effects of cryogenic treatment on tensile properties: A comparative study. *Composites Part B: Engineering*, 2018. **147**: p. 1. https://doi.org/10.1016/j.compositesb.2018.04.024.
[26] Wang, D.H., M. Ramulu,D. Arola, Orthogonal cutting mechanisms of graphite/epoxy composite. Part ii: Multi-directional laminate. *International Journal of Machine Tools and Manufacture*, 1995. **35**(12): p. 1639. http://dx.doi.org/10.1016/0890-6955(95)00015-P.